Title
AXIAL DISPERSION IN EXTRACTION COLUMN PERFORMANCE

Authors
Vermeulen, T.
Moon, J.S.
Hennico, A.
et al.

Publication Date
1966-09-01

UCRL-17160

University of California

Ernest O. Lawrence Radiation Laboratory

AXIAL DISPERSION IN EXTRACTION COLUMN PERFORMANCE

Berkeley, California

DISCLAIMER

Submitted to Chemical Engineering Progress

UCRL-17160
Preprint

UNIVERSITY OF CALIFORNIA

Lawrence Radiation Laboratory
Berkeley, California

AEC Contract No. W-7405-eng-48

AXIAL DISPERSION IN EXTRACTION COLUMN PERFORMANCE

T. Vermeulen, J. S. Moon, A. Hennico, and T. Miyauchi

September 1966

UCRL 12166

AXIAL DISPERSION IN EXTRACTION COLUMN PERFORMANCE

T. Vermeulen, J. S. Moon*, A. Hennico**, and T. Miyauchi***
University of California, Berkeley, California

Abstract

Axial dispersion in one or both counterflowing phases can reduce the extraction performance of differentially continuous columns by a substantial extent. Entrainment between mixing stages of a compartmented system has a similar effect, possibly less pronounced. Theoretical treatments based on these two model systems are summarized, and are shown to be related; and the available calculation methods are identified.

Conventional analyses of mass transfer in extraction have generally ignored the dispersion behavior. Experimental columns should habitually be characterized by tracer runs, and also concentration profiles during steady-state extraction should be measured, in order to separate axial-dispersion and mass-transfer effects and to correlate the latter adequately.

This paper concludes with a review of typical dispersion parameters evaluated for six industrially useful types of extraction equipment.

*Moon-Myung Distillery, Seoul, Korea

**French Petroleum Institute, Rueil-Malmaison, France

***University of Tokyo, Tokyo, Japan

AXIAL DISPERSION IN EXTRACTION COLUMN PERFORMANCE

In the past fifteen years there has been growing awareness of the part played by axial dispersion in extraction column performance. The development of mechanical aids for phase dispersion and mass transfer -- specifically agitation, pulsation, and potentially ultrasonic or other vibration -- has made it amply evident that fluid-mechanical aspects of column operation will limit the performance in cases where the mass-transfer rates are high.

Axial (or longitudinal) dispersion, the main subject of this review, describes a group of local effects which in principle occur uniformly along the path of the countercurrently flowing liquids. Large-scale maldistribution of flow, or "channeling," is a different effect, in the present authors' view, and should be accounted for separately. So, also, are the "end effects" which lead to mixing and mass-transfer effects of a type not characteristic of the rest of a column. Nonuniformity of composition in either flowing phase may be sustained by the slowness of transverse dispersion, a factor which will not be considered here.

Pratt (21), Giankoplis and Hixson (5), and Gier and Hougen (6) were among the earliest workers to recognize the effects of axial dispersion upon extraction efficiency. In their studies and in subsequent work, it has been necessary to consider the manner in which concentration patterns in a column vary from the profiles predicted by simple mass-transfer or equilibrium theories. The typical theoretical effect of axial dispersion upon mass

transfer is indicated in Figure 1 (17). This diagram can be considered to compare two different packed columns, each with 1.3 effective overall transfer units and with an "extraction factor" or capacity ratio (Λ) of 0.8, one column operating in ideal piston flow (giving the dashed curves) and the other operating with a moderate extent of axial dispersion (shown by the solid curves). In the latter, axial dispersion markedly lowers the mean driving potential for mass transfer (identified by heavy cross-hatching); hence a larger number of "true" transfer units is required than if no longitudinal mixing occurred (3.0 transfer units, rather than 1.3). The abrupt change or "jump" in concentration of each incoming stream as it enters the column, and the need to include transport by axial dispersion in material balances involving an internal cross-section of the column, are distinguishing effects. For staged flow, both sets of curves would be stepped; they would lie in the same relative locations, but with the backflow (dispersion) case showing a larger number of steps.

Two approaches have been adopted for describing extraction columns. The first of these (17,22) is based on a differentially continuous column or "diffusion model," typified by a packed column with moderately small packing. The assignable parameters of the system in this case, in addition to the true NTU, are the $(N_{ox})_\lambda$ axial-dispersion coefficients (E) or column Péclet numbers (designated P_xB, with P_x the local Péclet number and B the ratio of column length to the local characteristic dimension.) The other approach (the "back-flow" model) is based on individual stages, either at equilibrium or possessing a finite mass-transfer rate, with a reverse flow of each stream from each given stage to

respective
the/adjacent stage (18,23). The controlling variables are now the back-flow ratios α_x ($= F_x / \bar{F}_x$) and α_y ($= F_y / \bar{F}_y$), the total true NTU (designated N_{ox}), and the number of stages n_s. If N_{ox} is very large, then each stage is essentially in equilibrium, and the system is described by three parameters having a one-to-one correspondence to (but not identity with) the parameters of the differential model. That is, n_s, α_x, and α_y replace N_{ox}, P_xB, and P_yB.

This paper will deal in large part with the potential uses of these two models in the interpretation and correlation of experimental data and in the design of new columns. For "long" columns the models are relatively interchangeable. Theoretically the diffusion model is more appropriate for packed or spray columns. The back-flow model should be preferable for sieve-plate columns with or without pulsation, and for rotating-disc contactors (25) and Rushton ("Mixco") columns (19) in which discrete stages are formed by the mixing that occurs between annular "doughnut" baffles in contact with the column wall and open centrally; in such apparatus, however, the effective number of stages may range between half and twice the actual number.

Only countercurrent operations involving a single solute will be considered here. The main purpose of this paper is to outline the simplest possible conditions for calculating the effects of axial dispersion upon solvent extraction. Types of problems that can be solved without machine computation will be considered -- those involving uniform flows and backflows or uniform axial-dispersion coefficients; constant or linearly varying partition coefficients; and uniform mass-transfer coefficients or stage heights, or both. Where these conditions are not maintained,

a finite-difference or stage-by-stage computation should be carried out, modeled upon the extraction programs of Hanson and coworkers (7, 8) but with added provision for mass-transfer rate, and for recycle flow or axial-dispersion transport.

Diffusion Model

A generalized mathematical treatment is used, which provides the greatest possible access to previously calculated numerical solutions. The pertinent variables are:

1. Relative solute concentrations X and Y, defined to lie within the range of 0 to 1. X applies to the feed phase or raffinate, Y to the solvent phase or extract. These are taken as the average values at the cross-section of interest, so that the problem can be treated as being one-dimensional in its space variables. The feed enters at X (= X^0) = 1, and the solvent at Y (= Y^1) = 0. In terms of the true concentrations c_x and c_y, the generalized concentrations are

$$X = \frac{c_x - (q + mc_y^1)}{c_x^0 - (q + mc_y^1)} \tag{1}$$

$$Y = \frac{mc_y - mc_y^1)}{c_x^0 - (q + mc_y^1)} \tag{2}$$

Here superscript 0 represents the feed inlet end, and superscript 1 the solvent inlet end, both outside the column. Also, q is the intercept on a linear equilibrium plot, and m is the slope of the plot, such that the equilibrium value $(c_x)^*$ is given by

$$\left.\begin{aligned} (c_x)^* &= q + mc_y \\ (X)^* &= Y \end{aligned}\right\} \tag{3}$$

2. Capacity ratio or extraction factor Λ, with

$$\Lambda = m\overline{F}_x / \overline{F}_y \tag{4}$$

where $\overline{F}_x$ and $\overline{F}_y$ are the superficial velocities of the X and Y phases; Λ is the reciprocal of the factor KS/H used by Pigford (20).

3. A "column Péclet number" for each phase: P_xB, P_yB. Here P_i (with i = x or y) is the local Péclet number, given by the ratio of a characteristic local length d to the effective "mixing length" ℓ. In turn, the latter is the ratio of a superficial axial-dispersion coefficient E_i to the superficial velocity $\overline{F}_i$. Also, B is the ratio of total column height L to the local length d. Thus,

$$P_iB = \frac{L}{\ell_i} = \frac{\overline{F}_i L}{E_i} \tag{5}$$

The dispersion coefficient is a probabilistic term accounting primarily for velocity distribution effects, including eddy mixing and interphase entrainment.

4. The number of true overall mass-transfer units relative to the X phase (N_{ox}), based upon the mass-transfer coefficient (k_{ox}) and the interfacial area per unit volume (a):

$$N_{ox} = k_{ox} a h / \overline{F}_x \tag{6}$$

5. The fractional length within the column (Z), as a ratio of distance from the feed-input end (z) to the total column length (h):

$$Z = z / h \tag{7}$$

For the two phases, the diffusion equations are then written

$$\left.\begin{aligned} \frac{d^2X}{dZ^2} - P_xB\frac{dX}{dZ} - N_{ox}P_xB\,(X - Y) &= 0 \\ \frac{d^2Y}{dZ^2} - P_yB\frac{dY}{dZ} + \Lambda N_{ox}P_yB\,(X - Y) &= 0 \end{aligned}\right\} \qquad (8)$$

Solutions

The algebraic and numerical solution of these equations has been reported by Sleicher (22) and by Miyauchi, McMullen, and Vermeulen (14,17). It is evident that they are in the form:

$$\begin{aligned} X &= Y(N_{ox},\ \Lambda,\ P_xB,\ P_yB,\ Z) \\ Y &= Y(N_{ox},\ \Lambda,\ P_xB,\ P_yB,\ Z) \end{aligned} \qquad (9)$$

Computed X and Y profiles are known (14) for about 750 sets of values of the four independent parameters N_{ox}, Λ, P_xB, and P_yB. The values for X^1 (or X_1), the solute fraction in the exit raffinate, are of greatest interest; the computed values have been used to develop an approximate calculation method for X^1 in terms of the four parameters, which is described below. We note that the extract concentration Y^0 (or Y_0) is also of major interest, but is readily obtainable by material balance:

$$Y^0 = \Lambda(1 - X^1) \qquad (10)$$

It is appropriate now to relate the four-parameter results to a succession of simpler situations.

The One-Parameter System: Λ Finite. Here perfect mass transfer and negligible axial dispersion are assumed; that is, $P_xB = \infty$, $P_yB = \infty$, and $N_{ox} = \infty$ (hence, $X = Y$ at each point). We then find:

$$\left.\begin{array}{lll} \text{For } \Lambda \leq 1 & X^1 = 0; & Y^0 = \Lambda \\ \text{For } \Lambda \geq 1 & X^1 = (\Lambda - 1)/\Lambda; & Y^0 = 1 \end{array}\right\} \quad (11)$$

A Two-Parameter System: Λ and N_{ox} Finite. Again axial dispersion is neglected, which gives rise to the Colburn equation (2):

$$X^1 = \frac{1 - \Lambda}{\exp\left[(1 - \Lambda)N_{ox}\right] - \Lambda} \quad (12)$$

A Three-Parameter System: Λ, P_xB and P_yB Finite. This time, perfect mass transfer is assumed ($N_{ox} = \infty$), and again a simple analytic result is obtained:

$$X^1 \ (=Y_1) = \frac{\Lambda - \Lambda^2}{\exp\left[(1 - \Lambda)P_{oy}B\right] - \Lambda^2} \quad (13)$$

where $P_{oy}B$ is an overall column Péclet number, given by

$$P_{oy}B = \left[\frac{\Lambda}{P_xB} + \frac{1}{P_yB}\right]^{-1} \quad (14)$$

Figure 2 is a plot of Equation 13. The solution is independent of whether axial dispersion occurs in the extract phase, the raffinate phase, or both.

The "jump" behavior at the Y-phase inlet is measured by Y_1, above, since $Y^1 = 0$. The "jump" at the feed inlet is given by $1 - X_0$, where

$$X_0 \ (=Y^0) = \frac{\Lambda \exp\left[(1 - \Lambda)P_{oy}B\right] - \Lambda^2}{\exp\left[(1 - \Lambda)P_{oy}B\right] - \Lambda^2} \quad (15)$$

A "jump ratio" r, useful in determining $P_{oy}B$ from experimental

concentration profiles, is defined for each phase as the ratio of the concentration change at the inlet to the total concentration change in that phase:

$$\left.\begin{aligned} r_x &= (1 - X_0) / (1 - X^1) \\ r_y &= Y_1 / Y^0 \end{aligned}\right\} \qquad (16)$$

Here X_0 and Y_1 are the "interior" column concentrations, after the "jumps" from X^0 and Y^1 have occurred. At the outlet for each stream, no jump occurs.

It should be noted that an inlet "jump" may occur <u>even without axial dispersion</u>. From Equation 11 with $\Lambda \leq 1$, $X_0 = \Lambda$, and $r_x = 1 - \Lambda$; with $\Lambda \geq 1$, $Y^1 = r_y = 1 - (1/\Lambda)$. Figure 3 shows the behavior of the "jump ratios" at $N_{ox} = \infty$, with the $P_{oy}B$ contours ranging from 0 in the upper right corner to ∞ along the left-hand side and bottom of the plot.

<u>Three-Parameter Case: Λ, N_{ox} and P_xB or P_yB Finite</u>. This case, with axial dispersion absent in one phase, corresponds to certain packed and spray columns where the discontinuous phase may undergo almost no axial mixing. It has been explored by Eguchi and Nagata (<u>4</u>), and the analytical solution is listed in Miyauchi and Vermeulen's summary (<u>17</u>). Tables of concentration profiles for this case, in a form to match the available four-parameter tables, have recently been computed (<u>27</u>).

<u>Approximate Treatment for the Four-Parameter System</u>. An apparent (or "piston-flow") NTU (= N_{oxP}), replacing N_{ox} in Equation 12, is defined in relation to X^1:

$$N_{oxP} = \frac{1}{1-\Lambda} \ell n \left\{ \frac{1-\Lambda}{X^1} + \Lambda \right\} \tag{17}$$

Comparison of Equations 12 and 13 indicates that, at $N_{ox} = \infty$,

$$(N_{oxP})_{N_{ox}=\infty} = P_{oy}B + \frac{\ell n \Lambda}{\Lambda - 1} \tag{18}$$

An overall number of dispersion units N_{oxD} is therefore defined and related to N_{oxP}:

$$\frac{1}{N_{oxD}} \equiv \frac{1}{N_{oxP}} - \frac{1}{N_{ox}} \tag{19}$$

with

$$N_{oxD} = (PB)_y + \frac{\ell n \Lambda}{\Lambda - 1} \tag{20}$$

and

$$(PB)_y \equiv \left[\frac{\Lambda}{f_x P_x B} + \frac{1}{f_y P_y B} \right]^{-1} \tag{21}$$

The weighting factors f_x and f_y are empirical functions of N_{ox} and Λ, evaluated from the computed solutions of Equations 8, and plotted in Figure 4. (Equation 20 should not be used in the form given here if either ΛN_{ox} or $(PB)_y$ is less than unity.) Through these approximate relations X_1 and N_{oxP} are expressed as quite simple functions of the four independent parameters.

A closely related type of explicit approximation has been developed by Stemerding and Zuiderweg (24).

The design of a column requires a knowledge of Λ, and estimates of N_{ox}, P_x, and P_y. The interpretation of column runs requires that P_xB and P_yB be determined either from "jump ratio" plots (17) or from separate unsteady-state experiments (9), so that N_{ox} may be deduced from the experimental N_{oxP}.

End effects in columns, due to different rates of mass transfer or dispersion from those in the main body of a column, have been treated in the context of axial dispersion-- theoretically by Wilburn (29) and Tomura and Miyauchi (26), and empirically by Moon et al. (15).

Backflow Model

Figure 5 shows the flows to be considered in a cell model with recycle flows, which for instance corresponds to a multistage mixer-settler extractor with interstage entrainment. Again $\overline{F}_x$ and $\overline{F}_y$ are the net superficial velocities of phases X and Y through the column; F_x and F_y are the recycle flows, which must each occur in both directions but with each phase having different compositions in the two directions; and α_x and α_y are the recycle ratios, given by $F_x / \overline{F}_x$ and $F_y / \overline{F}_y$. The number of stages is n_s, the height per stage is h_S, and the fractional height per stage is $h_S / h = L_S = 1/n_s$. The total true NTU in the column being again given by Equation 6, the NTU per stage is

$$N_{oxS} = k_{ox} a \, h_S / \overline{F}_x \tag{22}$$

The material balance and the rate within each stage combine to give the following relations, expressed here for stage j:

$$\left.\begin{aligned} (1-\alpha_x)(X_{j-1} - X_j) - \alpha_x(X_j - X_{j+1}) - N_{oxS}(X_j - Y_j) &= 0 \\ (1+\alpha_y)(Y_j - Y_{j+1}) - \alpha_y(Y_{j-1} - Y_j) - N_{oxS}(X_j - Y_j) &= 0 \end{aligned}\right\} \tag{23}$$

For the end stages, the material balances are simpler. For example, at $j = 1$,

$$(X^0 - X_{(1)}) - \alpha_x(X_{(1)} - X_{(2)}) - N_{oxS}(X_{(1)} - Y_{(1)}) = 0$$

$$(1 + \alpha_y)(Y_{(1)} - Y_{(2)}) - N_{oxS}(X_{(1)} - Y_{(1)}) = 0$$

Any solution to the general problem would be expressed in the form

$$\left.\begin{aligned} X &= X(n_s,\ N_{oxS},\ \Lambda,\ \alpha_x,\ \alpha_y,\ j) \\ Y &= Y(n_s,\ N_{oxS},\ \Lambda,\ \alpha_x,\ \alpha_y,\ j) \end{aligned}\right\} \quad (24)$$

The types of solution available for these equations will be reviewed here. Again, the outlet concentrations X^1 (= X at $j = n_s$) and Y^0 (= Y at $j = 1$) are of primary interest.

The One-Parameter System. For $j = n_s$, four other parameters must be defined, leaving Λ undefined: N_{oxS} is finite or infinite, $n_s = \infty$, $\alpha_x = 0$, $\alpha_y = 0$. The solutions are necessarily those given in Equations 11.

A Two-Parameter System: Λ and n_s Finite. Now $N_{oxS} = \infty$, and axial dispersion is neglected ($\alpha_x = 0$, $\alpha_y = 0$), giving rise to the usual Kremser equation (11):

$$X^1 = \frac{1 - \Lambda}{\Lambda^{-n_s} - \Lambda} \quad (25)$$

A Three-Parameter System: Λ, α_x, and α_y Finite. Now $n_s = \infty$, and N_{oxS} may be finite or infinite. Using the result for the next case below, it can be shown that infinite n_s overcomes any extent of interstage backflow, and hence that the result is the one just given for the one-parameter system.

Finite α's are thus seen to be analogous to finite local Péclet numbers. For a column of infinite length, the column Péclet numbers become infinite, even though the axial-dispersion coefficients and the local Péclet numbers remain finite.

A Four-Parameter System: Λ, n_s, α_x, and α_y Finite. For this case, with $N_{oxS} = \infty$, Sleicher (23) has given the solution:

$$X^1 = \frac{\Lambda - \Lambda^2}{\Gamma^{1-n_s} - \Lambda^2} \tag{26}$$

with

$$\Gamma = \frac{\Lambda\alpha_x + \alpha_y + \Lambda}{\Lambda\alpha_x + \alpha_y + 1} \tag{27}$$

We note that interstage entrainment reduces the effective number of equilibrium contacts, which may be designated n_s^*. Comparison of Equations 25 and 26 yields the result:

$$\Lambda^{1-n_s^*} = \Gamma^{1-n_s} \tag{28}$$

Since Γ always lies between Λ and 1, n_s^* is always less than n_s.

Five-Parameter System: Λ, n_s, N_{oxS}, α_x and α_y Finite. Sleicher (23) has provided an empirical relation for this case, to be used with Equation 26. A slightly modified form is:

$$\Gamma \approx \frac{\Lambda\alpha_x + \alpha_y + \Lambda + (1/N_{oxS})}{\Lambda\alpha_x + \alpha_y + 1 + (1/N_{oxS})} \tag{29}$$

A comparison between the two models is given by the Latinen-Stockton equation (12,18), written for each phase:

$$P_i B = \frac{n_s - 1}{\alpha_i + 0.5} \tag{30}$$

Strictly, this relation applies only at infinite N_{oxS} and N_{ox}. For finite values of the latter, it appears appropriate to set $N_{ox} = n_s N_{oxS}$. For calculations at $(\Lambda\alpha_x + \alpha_y)$ below 1.0, the right-hand side of Equation 30 is multiplied by a factor f_T (18), this being given by

$$f_T = (\tfrac{1}{2} + \Psi)\ \ell n\ (1 + \tfrac{1}{\Psi}) \tag{31}$$

with $\Psi = [\Lambda + (\Lambda\alpha_x + \alpha_y)] / (1 - \Lambda)$.

At large α and large n_s, the axial-dispersion coefficient for a given phase can be associated with the product of the recycle flow and the stage height, h_S. A more complete relation, obtained from Equation 30, is:

$$E_i \approx \frac{h_S \alpha_i \bar{F}_i}{f_T} \left(1 + \frac{1}{2\alpha_i} + \frac{1}{n_s} \right) \qquad (32)$$

It should be noted that Equation 29 satisfies the limiting condition of $\alpha_x = 0$, $\alpha_y = 0$. The accuracy given by that equation for high extents of extraction (low X^1) may deserve further study. At $\Lambda = 1$, non-exponential relations replace Equations 12, 13, 15, 25, and 26 (18,23).

General Considerations

The diffusion model fits the spreading that occurs in the unsteady-state breakthrough of a tracer, whether this spreading is caused by velocity distribution, or mixing cells (either of these corresponding roughly to a one-directional random-walk behavior) or by entrainment by a counterflowing phase. This last, back-flow, effect can be separated from the forward-flow behavior by measurements upstream of a tracer injection point; but empirically it seems not to have any independent effect upon extraction behavior in a packed or spray column. That is, even though the axial dispersion is not symmetric and is therefore not represented exactly by a single effective diffusion coefficient, the same value of the coefficient that describes the forward spreading appears also to describe the downgrading of the solute-concentration profile, for extraction operations

conducted in the same apparatus under the same flow conditions as used for obtaining the spreading data.

In the backflow model, that part of the total spreading not due to backflow is attributed to mixing cells of appropriate size, each with its (constant) NTU. For a packed column in countercurrent flow, with both spreading and backflow measured for each stage, it is conceivable that the apparent number of mixing cells would not be the same for both phases. In that case the phase with less spreading (higher PB) could be treated inaccurately, having an α assigned to it that will match its total spreading but will disregard its true extent of backflow. No such column has yet had its backflow measured, since up to the present the data interpretation has emphasized the four-parameter diffusion model.

In a column with visible staging, if the concentration profiles during countercurrent flow are measured by sampling at many points, one can often discern concentration plateaus that identify the number of mixing cells. The number of structural stages n_p may be more or less than the effective number of mixing cells n_s.

Further computational studies are needed to improve the rules for conversions between the backflow and diffusion models. As mentioned above, the backflow model is generally more suitable for staged equipment and the diffusion model for differentially continuous systems.

Applications to Extraction Equipment

For the design and scale-up of extraction columns, it is necessary to have quantitative information, preferably in the form of dimensionless correlations based upon the fluid-mechanical factors that control the performance. This section describes the usable results that have come to the authors' attention; relatively few of all the extraction studies reported have included measurements of concentration profiles inside the column, or separate unsteady-state or tracer studies of the general mixing behavior. Six types of units will be reviewed here, of which two have been analyzed in terms of mixing cells with backflow.

Rotating-Disk Contactor. The RDC has been analyzed in substantial detail by Strand, Olney, and Ackerman (25). For the continuous phase these authors measured both backflow and spreading, and also mapped in detail the concentration patterns in individual stages of operating columns. If the number of partitioned compartments is taken as n_p, these authors find two effective stages per compartment throughout the range of useful flowrates and rotor speeds; that is, for the RDC,

$$\beta \equiv n_s / n_p = 2 \qquad (33)$$

With R designating the rotor diameter, D_T the column diameter, Ω the angular speed in revolutions per unit time, and $\bar{F}_i$ the superficial velocity of the liquid phase involved, the results of Strand et al. for each phase take the form

$$\alpha_i = 0.040\,[R\Omega/\bar{F}_i][R/D_T]^2 \qquad (34)$$

On the other hand, Miyauchi, Mitsutake, and Harase (16) have correlated these results with their own and other data, and have drawn different conclusions. They find, approximately,

$$\frac{\alpha \overline{F}}{\Omega R} = 0.005 \left(\frac{D_T}{h_S}\right)^{1/2} \left(\frac{D_r}{D_T}\right)^{7/4} \qquad (35)$$

where D_r is the inside diameter of the baffle ring between stages. The chief difference between these studies, yet to be completely resolved, lies in the question of the unmatched large dependences on D_r and on R.

Multicompartment Column with Agitation. This type of unit, known as the Mixco (Mixing Equipment Company) extractor, has been studied by Yagi, Miyauchi, and coworkers (16, 27). If the Reynolds number ($\Omega R^2/\nu$) is less than $1 \cdot 10^4$, $\beta = 2$ in Equation 33; if it is greater than about $2 \cdot 10^4$, $\beta = 1$. Their correlation is:

$$\frac{\alpha \overline{F}}{\Omega R} = \frac{0.020}{\beta} \left(\frac{D_T}{h_S}\right)^{1/2} \left(\frac{D_r}{D_T}\right)^{2} \qquad (36)$$

which they show is closely related to RDC behavior. In the narrow region where β is between 1 and 2, the correlating function (a type of Péclet group) rises more steeply with impeller size and speed. These results are for Mixco-type columns with four vertical baffles at the walls. Yagi and Miyauchi have measured E_i ($= \alpha_i \overline{F}_i D_T$) for columns without wall baffles, without doughnut baffles, and without either.

Yesterday Prof Treybal and Dr Bibaud reported their data on such columns. Cont. ph. OK; Disp. phase showed less Ax. Disp @ high $v_{disp.}$ or μ

Spray Towers. In spray columns the dispersed-phase droplets tend to approach plug-flow behavior, if they are uniformly sized and spaced so that no overtaking of droplets by one another occurs. The dispersed phase tends to entrain the continuous phase. For large density differences between phases, high viscosity ratios (of dispersed phase to continuous phase), and small height-to-diameter ratios, the

continuous phase may approach perfect mixing. Data of Gier and Hougen (6) and of Giankoplis et al. (5,10,26) have been analyzed, their columns ranging from 1.4 to 6.0 inches in diameter; the coefficient for the continuous phase has been found to fit the dimensional relation

$$E_c = 12\,(\overline{F}_d \cdot D_T)^{\frac{1}{2}} \qquad (37)$$

where both E_c and $\overline{F}_d D_T$ are expressed in cm^2/sec.

A slight possibility exists that the square-root of kinematic viscosity (ν_c) could be introduced to make this relation dimensionless. However, either a detailed fluid-mechanical analysis or further experimentation will be needed to show the influence of both physical properties and geometrical factors.

Pulsed Sieve-Plate Columns. Studies by Miyauchi and Ohya (16), by Mar and Babb (13), Burger and Swift (1), and Eguchi and Nagata (3) have indicated that Equation 32 can be applied to pulsed-column data, in the form:

$$E_i = \frac{h_P}{\beta}\left(\omega A + \frac{\overline{F}_i}{2}\right)$$

$$= 1.75\left(\frac{h_p}{D_T}\right)^{2/3} \frac{d_h}{s}\left(\omega A + \frac{\overline{F}_i}{2}\right) \qquad (38)$$

Here d_h is the effective diameter of perforations in the sieve plates, s is the fractional hole-area of the plates, ω is the frequency of pulsing, and A is the linear amplitude of the pulsation. The correlation given by Equation 37 is matched to continuous-phase data in Figure 6 and to dispersed-phase data in Figure 7.

It is of interest to compare the result of a linear-regression analysis by Mar and Babb. The terms for ωA and $\overline{F}_i$ were not separated as above, and this led to fractional exponents on those terms. Also, a lesser dependence upon hole diameter was reported, but interfacial tension (σ) appeared strongly as a factor:

$$E_c = (\text{const.})\ h_p^{0.68}\ \omega^{0.36}\ A^{0.07}\ d_h^{0.30}\ \sigma^{0.42}\ \overline{F}_d^{0.30} \Big/ \overline{F}_c^{0.45} \qquad (39)$$

The primary point of close agreement lies in the exponent on h_p. The influence of interfacial tension, in particular, is deserving of further study.

Packed Columns. Hennico, Jacques, and Vermeulen (9) have studied axial dispersion in packed columns involving a wide range of packing materials. Figure 8 gives their results in terms of packing Péclet number as a function of continuous-phase Reynolds number, flowrate ratio, and sphericity ψ and total void-fraction ϵ of the packing. Water was used as the continuous phase, and kerosene (or, in the cases marked by open squares, diisobutyl ketone) as dispersed phase. Density-difference effects have not been studied, and may enter into the eventual correlation; also, the effect of continuous-phase viscosity is inferred from dimensional considerations but has not yet been proved.

The dispersed phase is more difficult to measure, and only a few values of E_d have been obtained (by the same authors); however, extraction studies by Moon, Hennico, and Vermeulen (15)

confirm the relatively higher range of Péclet-number (or lower range of E_d) values. They are given here as the dashed curves in Figure 9.

Pulsed Packed Columns. Results similar to the above, for columns packed with Raschig rings or Berl saddles, have been obtained at several different pulse frequencies and amplitudes. Figure 10 shows these results on the same coordinates as for the data without pulsation (15).

We now find a substantial difference between Berl saddles and Raschig rings, not explained by the sphericity and void-fraction as used in the previous correlation.

The dispersed-phase Péclet-number values are again higher than those for the continuous phase, as shown from isolated experiments plotted in Figure 9.

Acknowledgment

The experimental results reported from this University were obtained in the Lawrence Radiation Laboratory, under the auspices of the U.S. Atomic Energy Commission. The authors are grateful to G. L. Jacques, J. E. Cotter, and N. N. Li for their contributions to the earlier portion of the experimental study.

Literature Cited

1. Burger, L. L., and W. H. Swift, U.S. Atomic Energy Comm., Hanford Works rept HW-29010 (1953).
2. Colburn, A. P., Trans. Am. Inst. Chem. Engrs. 29, 174 (1939); Ref. 20, p. 14-29.
3. Eguchi, W., and S. Nagata, Chem. Eng. (Japan) 22, 218 (1958).
4. Eguchi, W., and S. Nagata, Memoirs Fac. Engg., Kyoto Univ. 21, 70 (1959).
5. Geankoplis, C. J., and A. N. Hixson, Ind. Eng. Chem. 42, 1141 (1950).
6. Gier, T. E., and J. O. Hougen, ibid., 45, 1362 (1953).
7. Hanson, D. N., J. H. Duffin, and G. F. Somerville, "Computation of Multistage Separation Processes," Reinhold, New York (1962).
8. Hanson, D. N., and G. F. Somerville, Adv. Chem. Eng. 4, 279 (1963).
9. Hennico, A. N., G. L. Jacques, and T. Vermeulen, U.S. Atomic Energy Comm. rept. UCRL-10696 (1963).
10. Kreager, R. M., and C. J. Geankoplis, Ind. Eng. Chem. 45, 2156 (1953).
11. Kremser, A., Natl. Petr. News 22, no. 21, 42 (1930); ref. 20, p. 14-60.
12. Latinen, G. A., and F. D. Stockton, A.I.Ch.E. Natl. Meeting, St. Paul, Minn., Sept. 1959.
13. Mar, B. W., and A. L. Babb, Ind. Eng. Chem. 51, 1011 (1959).
15. Moon, J. S., A. N. Hennico, and T. Vermeulen, U.S. Atomic Energy Comm. rept. UCRL-10928 (1963).
14. McMullen, Alice, T. Miyauchi, and T. Vermeulen, U. S. Atomic Energy Comm. rept. UCRL-3911-Suppl. (1958).

16. Miyauchi, T., and H. Ohya, A.I.Ch.E. Journal 11, 395 (1965); T. Miyauchi, H. Mitsutake, and I. Harase, Ibid., accepted for publication.

17. Miyauchi, T., and T. Vermeulen, Ind. Eng. Chem. Fundls. Qtrly 2, 113 (1963).

18. Miyauchi, T., and T. Vermeulen, ibid. 2, 304 (1963).

19. Oldshue, J. Y., and J. H. Rushton, Chem. Eng. Progr. 48,

20. Pigford, R. L., in Perry's Chemical Engineers' Handbook, 4th ed., p. 14-60, McGraw-Hill, New York (1963).

21. Pratt, H. R. C., Trans. Inst. Chem. Engrs. (London) 29, 195 (1951).

22. Sleicher, C. A., A.I.Ch.E. Journal 5, 145 (1959).

23. Sleicher, C. A., ibid. 6, 529 (1960).

24. Stemerding, S., and F. J. Zwietering, Chem. Engr. (Inst. Chem. Engrs, London) 4, 156 (1963).

25. Strand, C. P., R. B. Olney, and G. H. Ackerman, A.I.Ch.E. Journal 8, 252 (1962).

28. Vogt, H. J., and C. J. Geankoplis, Ind. Eng. Chem. 46, 1763 (1954).

30. Yagi, S., and T. Miyauchi, Chem. Eng. (Japan) 19, 507 (1955).

26. Tomura, Yasushi, and T. Miyauchi, University of Tokyo, private communication.

27. Vermeulen, T., N. A. Leidel, and T. Miyauchi, U. S. Atomic Energy Comm., UCRL rept. in preparation.

29. Wilburn, N. P., Ind. Eng. Chem. Fundls. Qtrly. 3, 189 (1964).

Nomenclature

A - Pulse amplitude, cm

a - Interfacial area per unit bulk volume, cm^2/cm^3

B - Ratio of total length to characteristic local length (usually L/d_p), dimensionless

c_i - concentration of solute in ith phase, gram-moles/cc

d_p - Area-mean particle diameter, cm

D_T - Tower diameter, cm

F_i - Superficial volumetric backflow of ith phase through unit cross sections of apparatus, cm/sec

$\overline{F}_i$ - Superficial net forward volumetric flow rate of ith phase through unit cross section of apparatus, cm/sec

f_T - Correction factor for Equations 30 and 32, dimensionless

h - Height of one stage (h_s) or one compartment (h_p), cm

k - Over-all mass transfer coefficient

L - Effective column length in direction of mean flow, cm

ℓ_i - Mixing length, $E_i/\overline{F}_i$, cm

m - Solute partition coefficient, dc_x^*/dc_y, dimensionless

n - Number of stages (n_s) or compartments (n_p), dimensionless

N - Number of over-all transfer units in column, dimensionless

P_i - Local Péclet number for ith phase, d/ℓ_i, dimensionless

q - Intercept on linear equilibrium plot, $c_x = q + mc_y$, gram-moles/cm^3

R - Rotor or impeller diameter, cm

r_i - Jump ratio in ith phase (see Equation 16), dimensionless

X - generalized solute concentration in X phase (see Equation 1), dimensionless

Y - generalized solute concentration in Y phase (see Equation 1), dimensionless

Greek Letters

α_i - $F_i / \overline{F}_i$, dimensionless

β - n_s / n_p

Γ - Performance factor for one stage (see Equation 30), dimensionless

ϵ - Fractional void-volume in packing occupied by fluid phase, dimensionless

Λ - Capacity ratio, mF_x / F_y, dimensionless

ν - Kinematic viscosity, cm^2/sec

σ - Interfacial tension, dynes/cm

Ψ - Term in f_T (see Equation 31), dimensionless

ψ - Sphericity

Ω - Rotational speeds, revs./sec

Subscripts

c - Continuous phase

d - Dispersed phase

j - Stage number

o - Overall

p - Compartments; packing particle

P - Pertaining to one compartment

P - (in N_{oxP}) Piston-flow

s - Stages

S - Pertaining to one stage

x - Refers to feed (X) phase

y - Refers to solvent (Y) phase

(1), (2), ... - Stage number

0 - Feed inlet end, inside column

1 - Solvent inlet end, inside column

Superscripts

* - Equilibrium

0 - Feed inlet end, outside column

1 - Solvent inlet end, outside column

Captions for Figures

Figure 1. Illustrative concentration profiles in countercurrent extraction, calculated without (---) and with (——) longitudinal dispersion. $A = 0.8$, $N_{oxP} = 1.3$. For solid curves, $P_xB = 1.5$, $P_yB = 3$.

Figure 2. Limiting extent of approach to complete extraction, as given by diffusion model for infinite N_{ox}.

Figure 3. Jump ratios at X-phase and Y-phase inlets, from the diffusion model at infinite N_{ox}.

Figure 4. Weighting factors for Equation 21.

Figure 5. Schematic diagram of mixing cells, for countercurrent operation with backflows.

Figure 6. Longitudinal-dispersion coefficients for continuous phase, in pulsed perforated-plate columns.

Figure 7. Longitudinal-dispersion coefficients for dispersed phase, in pulsed perforated-plate columns.

Figure 8. Packing Péclet number for continuous phase, in packed columns.

Figure 9. Packing Péclet number for dispersed phase, in packed columns without (---) and with (——) pulsation.

Figure 10. Packing Péclet number for continuous phase, in pulsed packed columns.

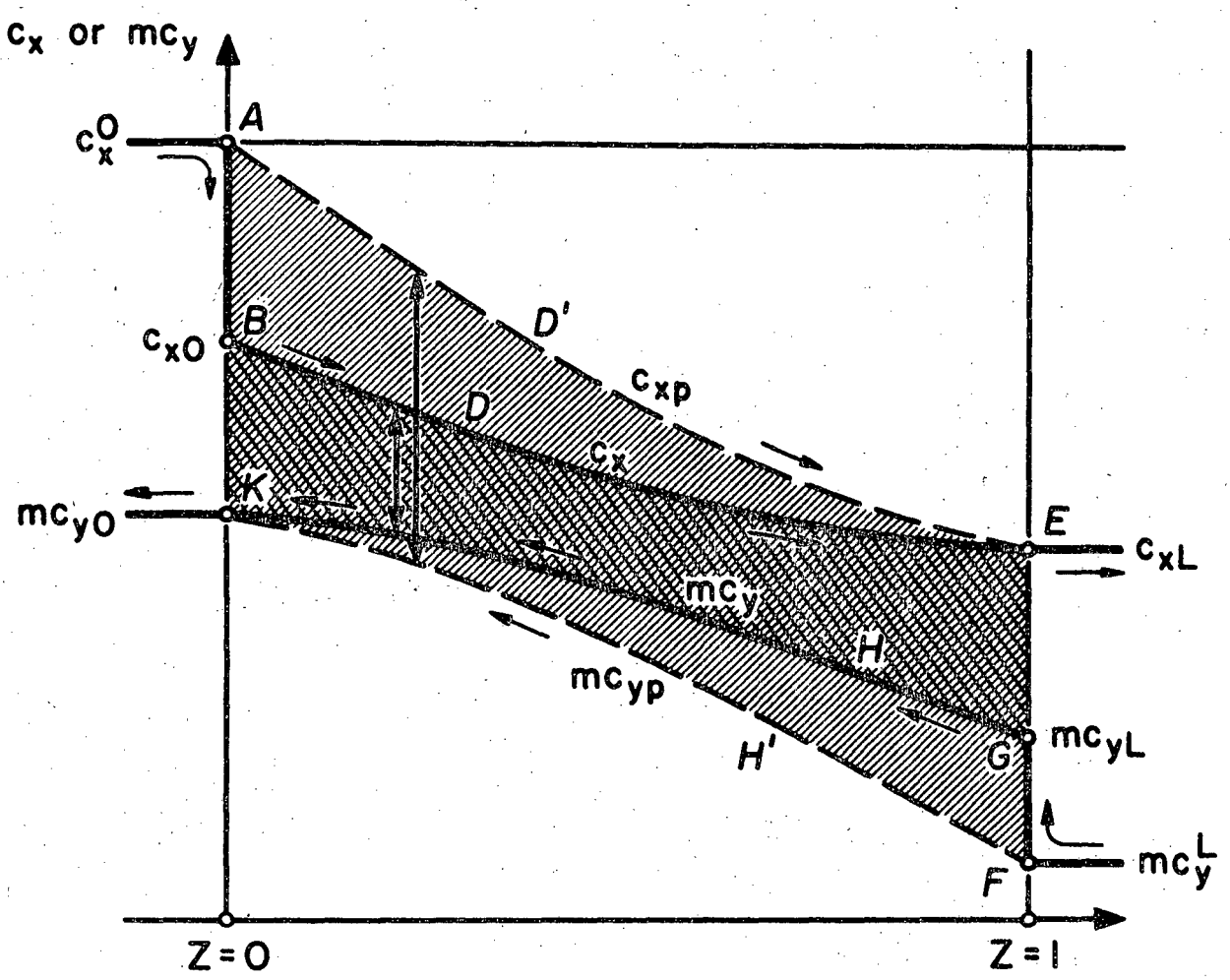

Figure 1. Illustrative concentration profiles in countercurrent extraction, calculated without (---) and with (——) longitudinal dispersion. $\Lambda = 0.8$, $N_{oxP} = 1.3$. For solid curves, $P_xB = 1.5$, $P_yB = 3$.

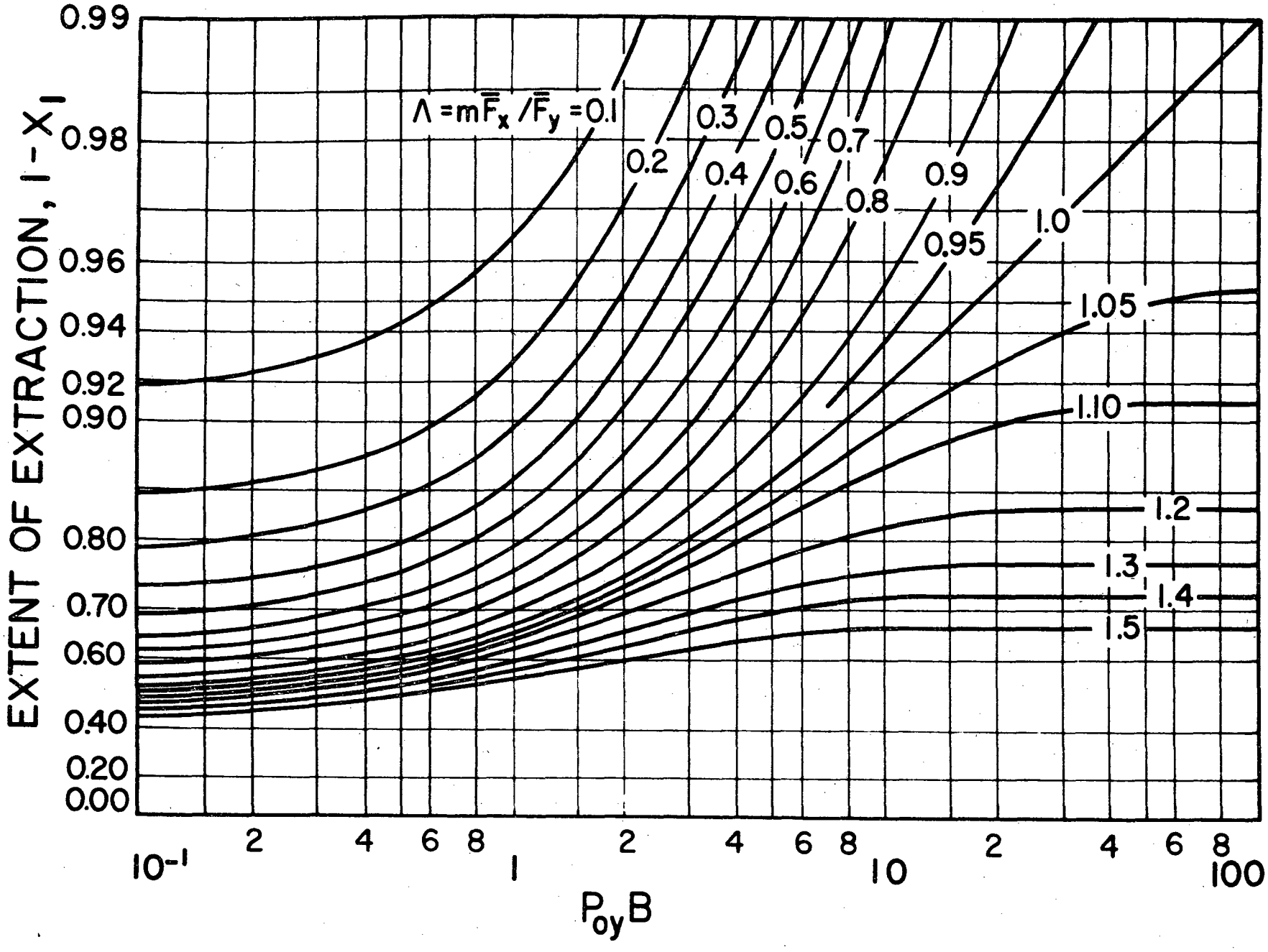

Figure 2. Limiting extent of approach to complete extraction, as given by diffusion model for infinite N_{ox}.

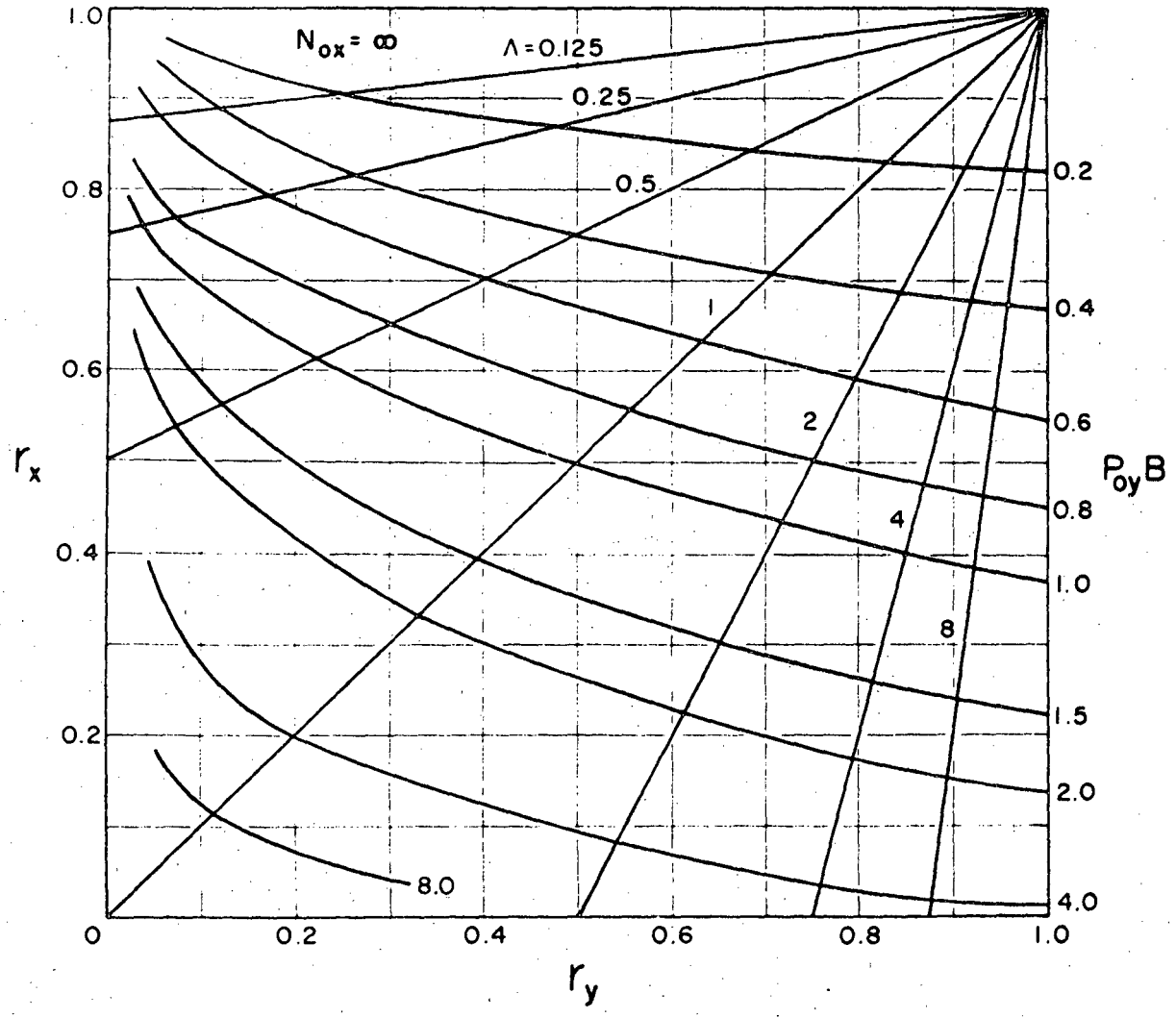

Figure 3. Jump ratios at X-phase and Y-phase inlets, from the diffusion model at infinite N_{ox}.

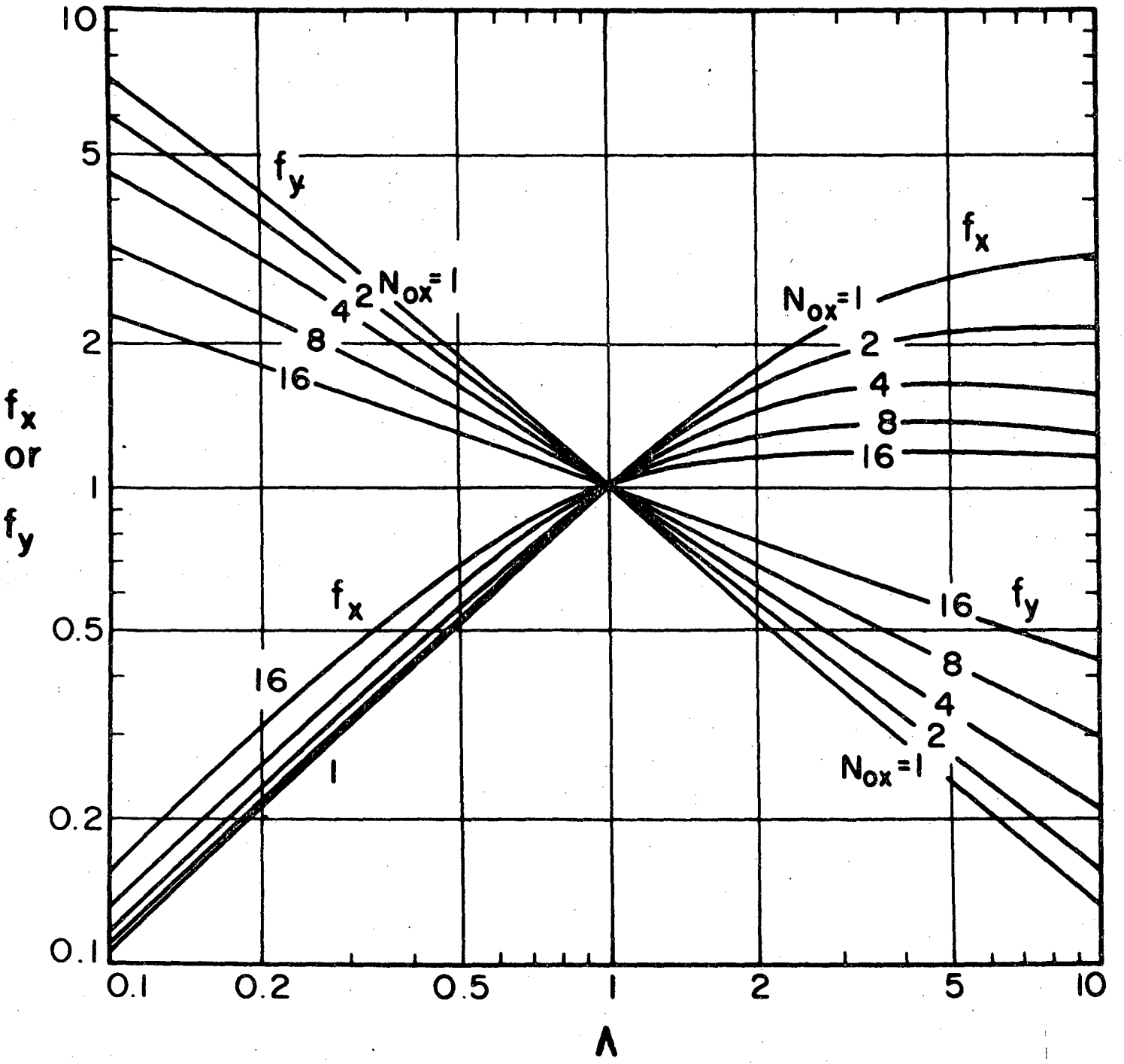

Figure 4. Weighting factors for Equation 21.

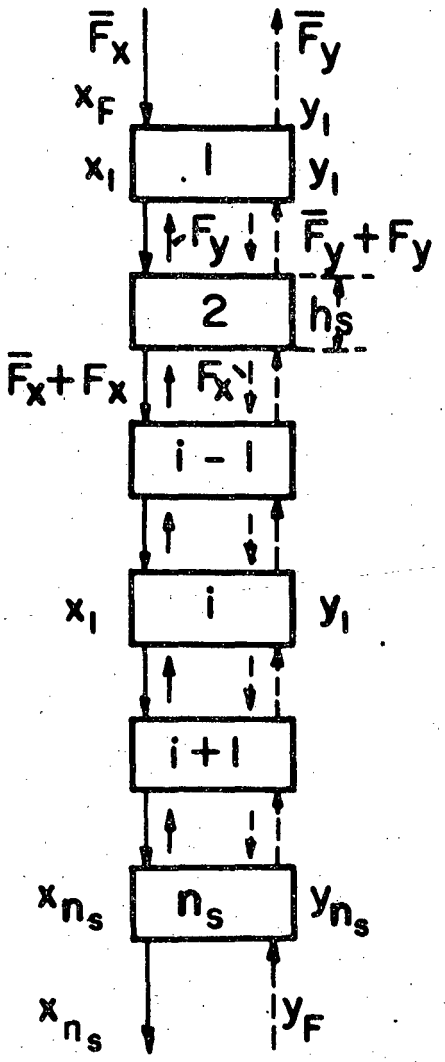

Figure 5. Schematic diagram of mixing cells, for countercurrent operation with backflows.

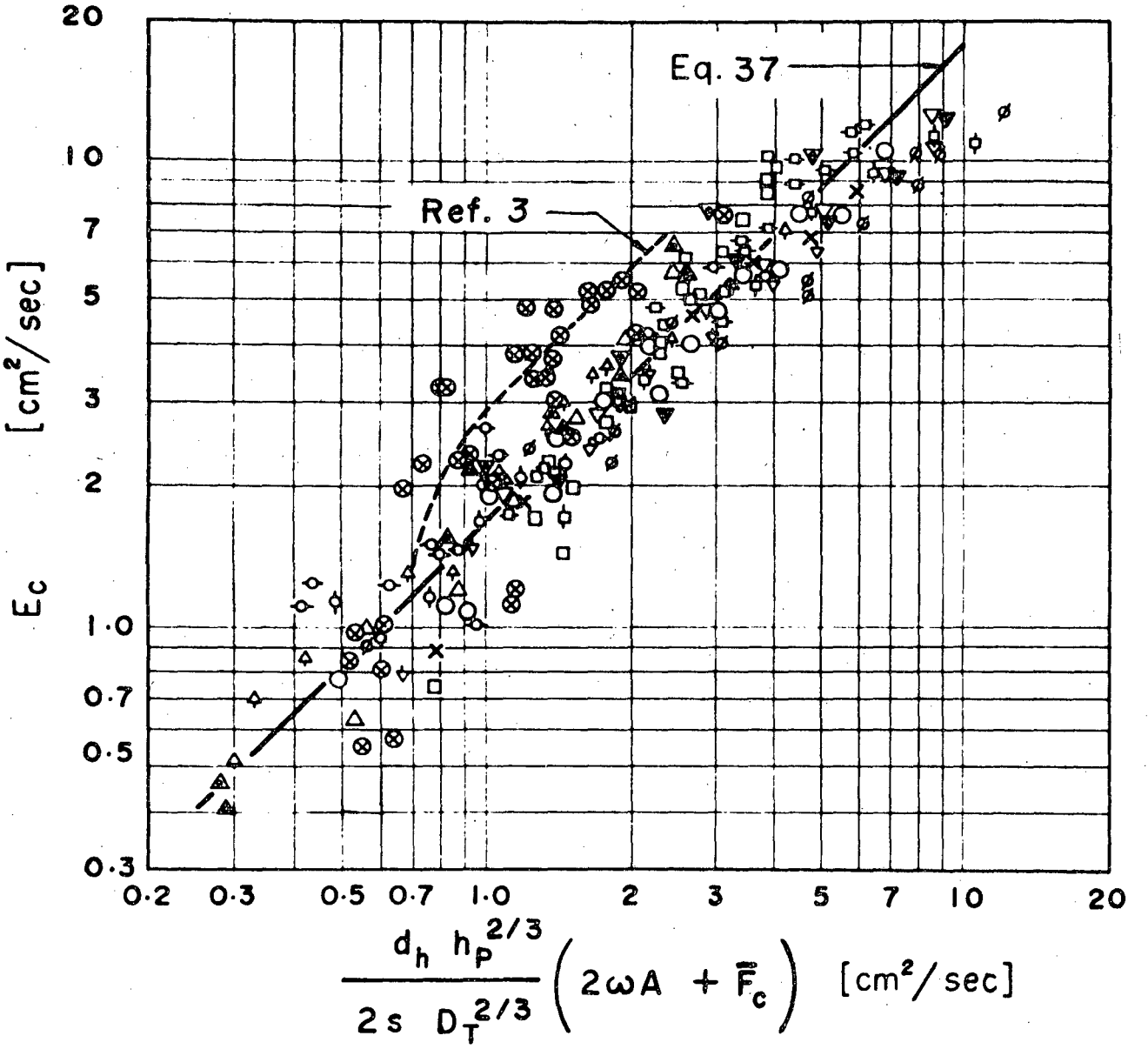

Figure 6. Longitudinal-dispersion coefficients for continuous phase, in pulsed perforated-plate columns.

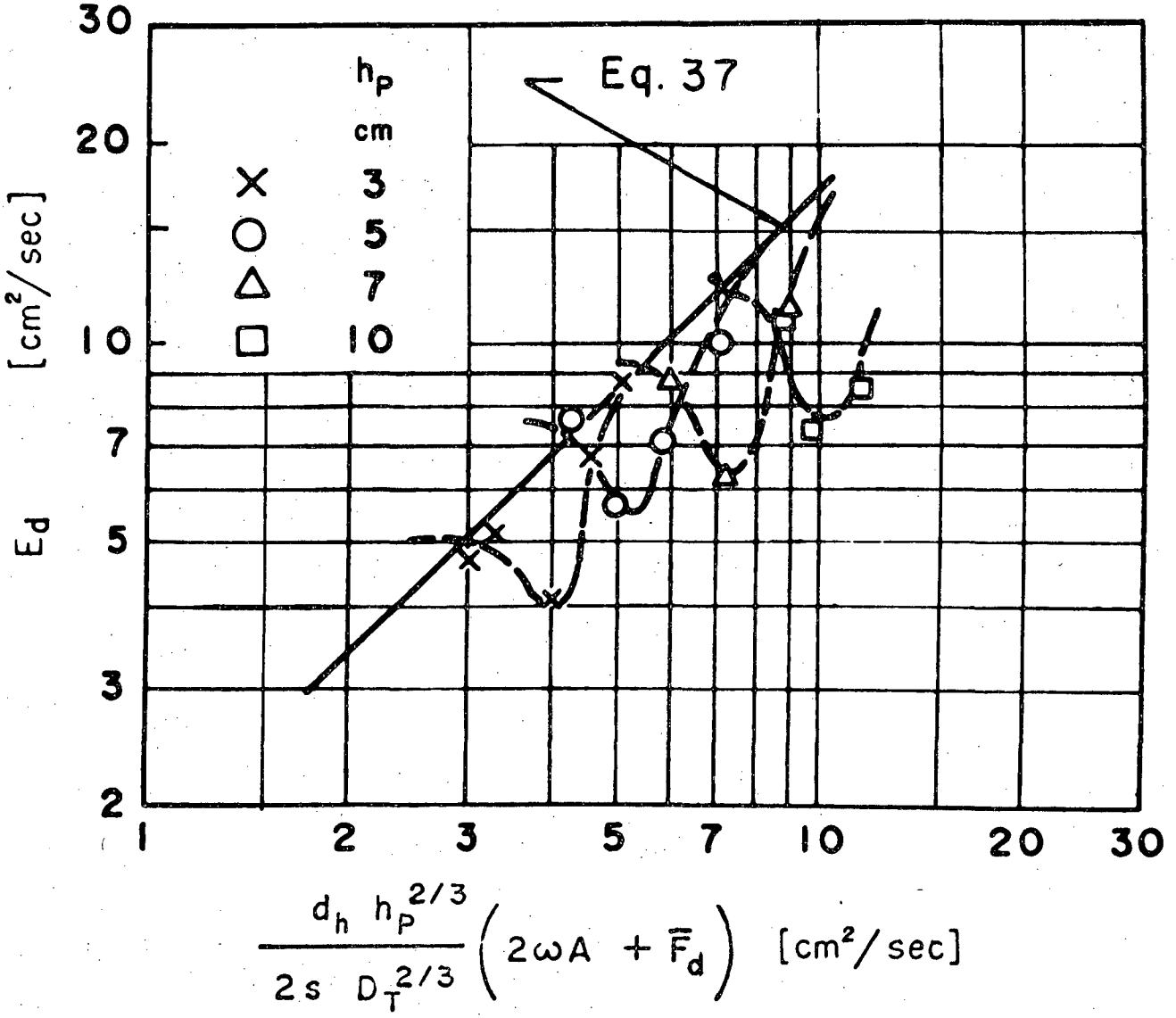

Figure 7. Longitudinal-dispersion coefficients for dispersed phase, in pulsed perforated-plate columns.

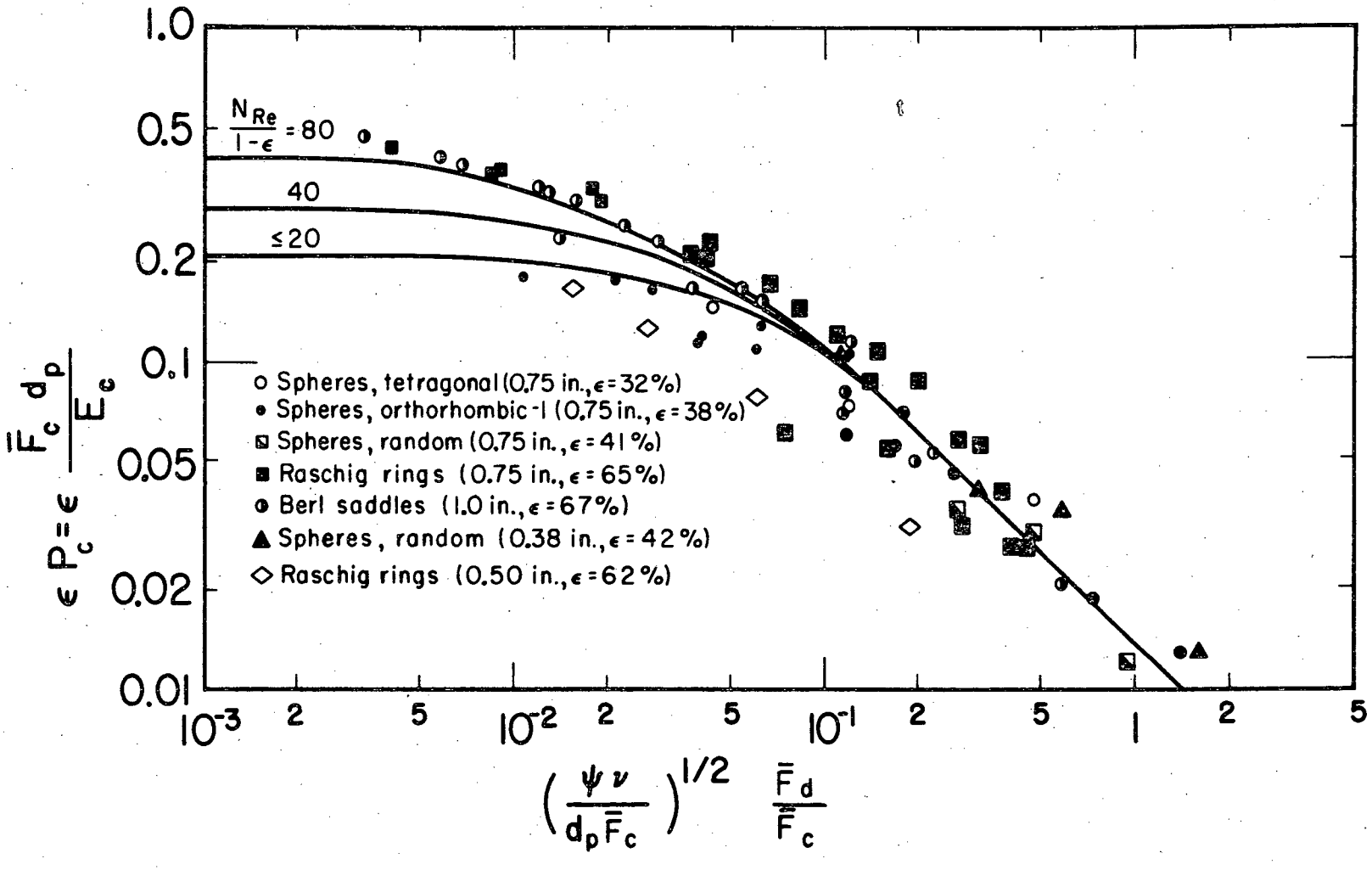

Figure 8. Packing Péclet number for continuous phase, in packed columns.

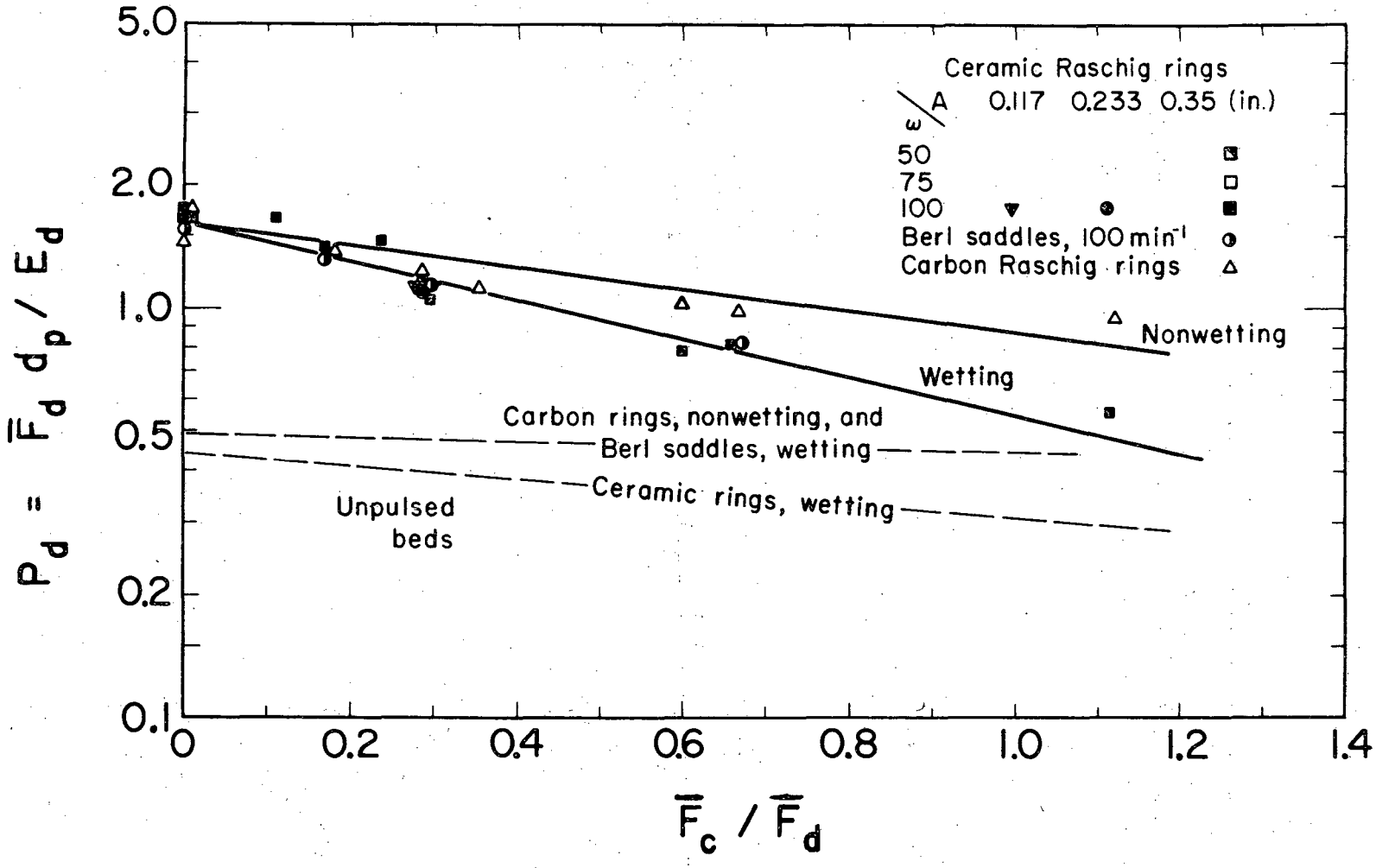

Figure 9. Packing Péclet number for dispersed phase, in packed columns without (---) and with (——) pulsation.

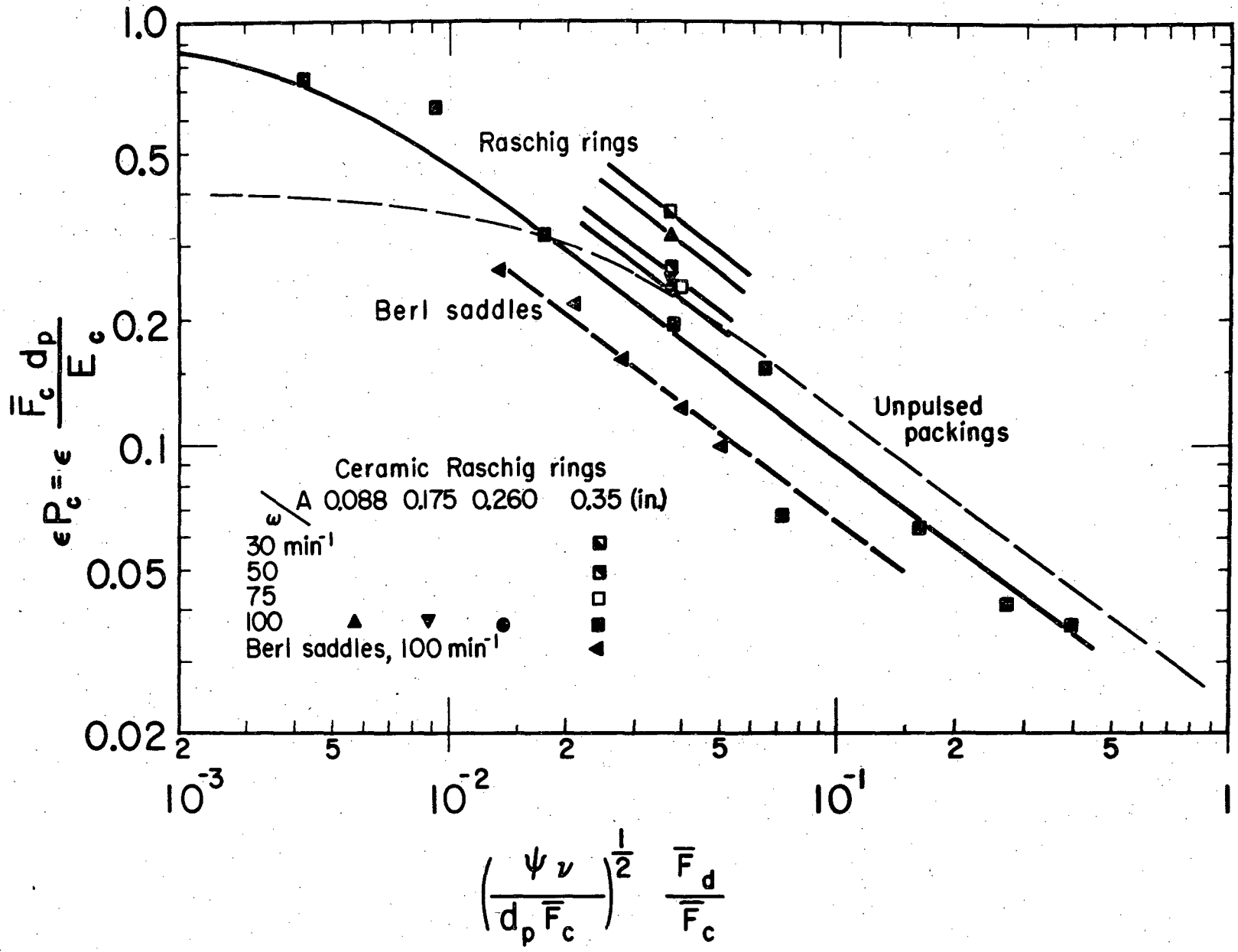

Figure 10. Packing Péclet number for continuous phase, in pulsed packed columns.